Supplementary material for "Anisotropic magnetoresistance in ferromagnetic atomic-sized metal contacts"

M. Häfner,[1,2] J. K. Viljas,[1,3] and J. C. Cuevas[2]

[1] *Institut für Theoretische Festkörperphysik and DFG-Center for Functional Nanostructures, Universität Karlsruhe, D-76128 Karlsruhe, Germany*

[2] *Departamento de Física Teórica de la Materia Condensada, Universidad Autónoma de Madrid, E-28049 Madrid, Spain*

[3] *Forschungszentrum Karlsruhe, Institut für Nanotechnologie, D-76021 Karlsruhe, Germany*

In this supplementary material we provide the details on our methods and present some further results. First, the tight-binding model and some numerical details are discussed. Then, we present a comparison of the results of ideal Ni contact to corresponding ones for the other $3d$ ferromagnetic materials Fe and Co. Finally, the minimal chain model is discussed in detail.

I. METHOD DETAILS

A. Tight-binding Hamiltonian with spin-orbit coupling

Our objective is to model the effect of spin-orbit coupling (SOC) on the transport in ferromagnetic atomic contacts. We start with the description of a ferromagnetic contact and introduce the SOC as a correction to the Hamiltonian of the ferromagnetic atomic contact. The Hamiltonian is thus of the single-particle form

$$\hat{H} = \sum_{i\alpha\sigma,j\beta\sigma'} (H^{(0)}_{i\alpha\sigma,j\beta\sigma'} + H^{(SO)}_{i\alpha\sigma,j\beta\sigma'})\hat{c}^{\dagger}_{i\alpha\sigma}\hat{c}_{j\beta\sigma'}, \tag{1}$$

where i, j denote the atomic site indices, α, β the different atomic orbitals, and $\sigma, \sigma' = \uparrow, \downarrow$ the spin, while $\hat{c}^{\dagger}_{i\alpha\sigma}$ ($\hat{c}_{i\alpha\sigma}$) are the associated electron creation (annihilation) operators. Here the elements without SOC form a matrix $\mathbf{H}^{(0)}$ that is diagonal in spin space

$$H^{(0)}_{i\alpha\sigma,j\beta\sigma'} = h^{(0)}_{i\alpha,j\beta;\sigma}\delta_{\sigma\sigma'}. \tag{2}$$

The elements $h^{(0)}_{i\alpha,i\alpha;\sigma}$ are the spin-dependent on-site energies, $h^{(0)}_{i\alpha,j\beta;\sigma}$ for $i \neq j$ are the hopping elements, while $h^{(0)}_{i\alpha,i\beta;\sigma} = 0$ for $\alpha \neq \beta$. For a nonorthogonal basis $|i\alpha\sigma\rangle$ we additionally need the spin-independent overlap integrals between different orbitals: $S_{i\alpha\sigma,j\beta\sigma'} = \langle i\alpha\sigma|j\beta\sigma'\rangle = s_{i\alpha,j\beta}\delta_{\sigma\sigma'}$. The creation and annihilation operators then satisfy $\{\hat{c}_{i\alpha\sigma}, \hat{c}^{\dagger}_{j\beta\sigma'}\} = [\mathbf{s}^{-1}]_{i\alpha,j\beta}\delta_{\sigma\sigma'}$. In the calculations of the realistic contacts, we use an atomic basis formed by the 9 orbitals $(3d, 4s, 4p)$, that give rise to the relevant bands around the Fermi energy of Fe, Co, and Ni. We take the parameters for $\mathbf{H}^{(0)}$ and $\mathbf{S}$ from the bulk parametrization of Refs. 1, 2, modifying $\mathbf{H}^{(0)}$ to satisfy charge neutrality. We note that the Hamiltonian $\mathbf{H}^{(0)}$ is symmetric: $(\mathbf{H}^{(0)})^t = \mathbf{H}^{(0)}$. The additional spin-orbit term $\mathbf{H}^{(SO)}$ couples the direction of the spin to the geometry and is assumed to be diagonal with respect to the site indices:

$$H^{(SO)}_{i\alpha\sigma,j\beta\sigma'} = h^{(SO)}_{i;\alpha\sigma,\beta\sigma'}(\theta,\phi)\delta_{ij}. \tag{3}$$

Here

$$h^{(SO)}_{i;\alpha\sigma,\beta\sigma'}(\theta,\phi) = \xi_i\langle i\alpha\sigma|\vec{\mathbf{l}}\cdot\vec{\mathbf{s}}|i\beta\sigma'\rangle = \frac{\xi_i}{2}\sum_{\mu,\nu} R_{\mu\nu}(\theta,\phi)l^{(\mu)}_{\alpha\beta}\tau^{(\nu)}_{\sigma\sigma'} \tag{4}$$

where ξ_i is the SOC constant on site i, $\mathbf{l}^{(\mu)}$ and $\boldsymbol{\tau}^{(\nu)}$ are the orbital momentum and the Pauli matrices, respectively, and $\mathbf{R}(\theta,\phi) = \mathbf{R}_z(\phi)\ \mathbf{R}_y(\theta)$ is a relative rotation between the spin and orbital quantization axes, where θ and ϕ are the polar and azimuthal angle. The $\mathbf{H}^{(SO)}$ matrix satisfies the time reversal symmetry $\left(\mathbf{H}^{(SO)}\right)^t(\theta,\phi) = \mathbf{H}^{(SO)}(\pi-\theta,\pi+\phi) = \boldsymbol{\tau}^{(2)}\mathbf{H}^{(SO)}(\theta,\phi)\boldsymbol{\tau}^{(2)}$. We only consider SOC on d orbitals, for which the the matrix elements [Eq. (4)] can be found in Ref. 3.

B. Conductance calculation

In order to calculate the current we use the standard nonequilibrium Green's function method [4–9]. Thus we divide the contact in three parts: the left (L) and right (R) leads and the central part (C) containing the atomic constriction. Neglecting direct coupling between (L) and (R) ($\mathbf{H}_{LR} = 0$ etc.), the retarded Green's function of the central part reads

$$\mathbf{G}_{CC}(\varepsilon, V) = \left[\varepsilon^{+}\mathbf{S}_{CC} - \mathbf{H}^{(0)}_{CC}(V) - \mathbf{H}^{(SO)}_{CC} - \mathbf{\Sigma}_L(\varepsilon - eV/2) - \mathbf{\Sigma}_R(\varepsilon + eV/2)\right]^{-1}, \tag{5}$$

where $\epsilon^{+} = \epsilon + i0^{+}$. Here we take into account the possibility that $\mathbf{H}^{(0)}$ may be voltage-dependent. The self energies $\mathbf{\Sigma}_X(\varepsilon)$ of lead X ($X = L, R$) contain the information about the coupling to the lead and can be written as:

$$\mathbf{\Sigma}_X(\varepsilon) = \left(\varepsilon\mathbf{S}_{CX} - \mathbf{H}^{(0)}_{CX}\right)\mathbf{g}_{XX}(\varepsilon)\left(\varepsilon\mathbf{S}_{CX} - \mathbf{H}^{(0)}_{CX}\right)^{\dagger}. \tag{6}$$

Again $\mathbf{H}^{(0)}_{CX}$ and $\mathbf{S}_{CX}$ are the hopping and overlap matrices between central part and lead $X = L, R$ and $\mathbf{g}_{XX}(\varepsilon)$ is the retarded surface Green's function of the uncoupled lead. The current through the constriction at finite bias V and temperature T takes the Landauer-Büttiker form

$$I(T, V) = \frac{e}{h}\int_{-\infty}^{\infty} d\varepsilon\, \tau(\varepsilon, V)\left[f(\varepsilon - eV/2, T) - f(\varepsilon + eV/2, T)\right], \tag{7}$$

where $\tau(\varepsilon, V) = \mathrm{Tr}\left[\mathbf{t}^{\dagger}(\varepsilon, V)\mathbf{t}(\varepsilon, V)\right]$ is the transmission function, $f(\varepsilon, T) = \{\exp[(\varepsilon - \varepsilon_F)/k_BT] + 1\}^{-1}$, is the Fermi function with Fermi energy ε_F and Boltzmann factor k_B, and

$$\mathbf{t}(\varepsilon, V) = \sqrt{\Gamma_L(\varepsilon - eV/2)}\mathbf{G}^{r}_{CC}(\varepsilon, V)\sqrt{\Gamma_R(\varepsilon + eV/2)}. \tag{8}$$

is the transmission matrix. The trace runs over site, orbital, and spin indices of the atoms coupled to the right lead. Here we introduced the positive definite "hopping rate" matrices $\mathbf{\Gamma}_X$ defined as:

$$\mathbf{\Gamma}_X(\varepsilon) = i[\mathbf{\Sigma}_X(\varepsilon) - \mathbf{\Sigma}^{\dagger}_X(\varepsilon)], \tag{9}$$

The nonlinear (differential) conductance is defined as $G(V) = dI/dV$ and the linear conductance is $G = G(V = 0)$. At zero temperature the linear conductance is given by the Landauer formula.

$$G = \frac{e^2}{h}\mathrm{Tr}[\mathbf{t}^{\dagger}(\varepsilon_F)\mathbf{t}(\varepsilon_F)] = \frac{e^2}{h}\sum_n \tau_n(\varepsilon_F). \tag{10}$$

Here the $\tau_n(\varepsilon)$ are the eigenvalues of $\mathbf{t}^{\dagger}(\varepsilon)\mathbf{t}(\varepsilon)$, i.e. the eigenchannel transmission probabilities

C. Anisotropic magnetoresistance

Due to SOC, the individual channel transmissions and thus the conductance depend on the angles θ and ϕ. This is the anisotropic magnetoresistance (AMR) effect, and we use this name, although we treat it in terms of the conductance instead of the resistance. It is now useful to make the following definitions. The mean conductance (linear or non-linear) averaged over the polar angle is

$$\langle G(\theta, \phi)\rangle_{\theta} = \int_0^{\pi} \frac{d\theta}{\pi}\, G(\theta, \phi) \tag{11}$$

and similarly the mean conductance averaged over all directions is given by

$$\langle G(\theta, \phi)\rangle_{\theta,\phi} = \int \frac{d\Omega}{4\pi}\, G(\theta, \phi). \tag{12}$$

The conductance variations are described, for example, by the relative conductance

$$G_{rel}(\theta, \phi) = \left[G(\theta, \phi) - \langle G(\theta, \phi)\rangle_{\theta}\right]/\langle G(\theta, \phi)\rangle_{\theta}. \tag{13}$$

For given ϕ we also define the amplitude of variation with θ, or AMR amplitude

$$\Delta G(\phi) = \max_{\theta}\left[G(\theta, \phi)\right] - \min_{\theta}\left[G(\theta, \phi)\right]. \tag{14}$$

The relative AMR amplitude for fixed ϕ is given by $\Delta G(\phi)/\langle G(\theta, \phi)\rangle_{\theta}$. Finally, we note that the time reversal symmetry implies that the conductance satisfies $G(\theta, \phi) = G(\pi - \theta, \pi + \phi)$.

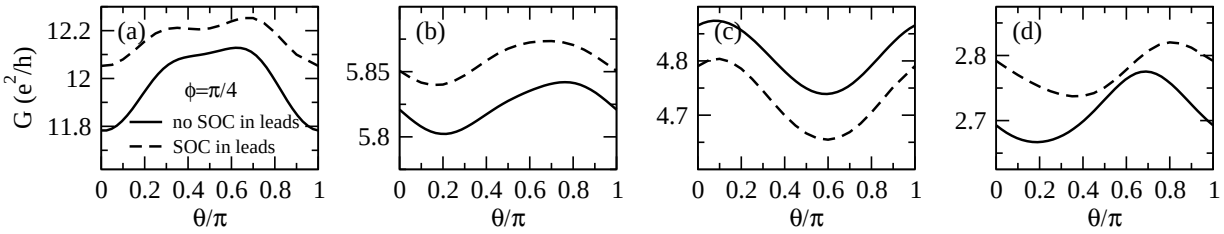

FIG. 1: (a)-(d) Comparison of conductance for geometries 1-4 for $\phi = \pi/4$ with and without SOC in the leads.

D. Numerical details

We calculate the surface Green's functions by using a Fourier transformation in the directions parallel to the surface and the decimation technique [10]. Without SOC, the only relevant energy scale in the problem is on the order of electronvolts. It is then sufficient to use energy broadenings as large as 0.5 eV in the leads and around 32^2 k points to converge the transmission functions. These calculations reproduce the results of Refs. 9, 11. In the presence of SOC however, the smallest energy scale that must be resolved is given by the SOC constant (70 meV in this work). In this case we obtain converged transmission results typically with a 10 meV energy broadening and 96^2 k points.

In principle SOC exists everywhere in the system, including the leads. Thus in the conductance calculations, one should separately evaluate the self energies for every angle pair (θ, ϕ). The computational effort can be considerably reduced by neglecting the SOC in the leads, and if the C region is large enough, the errors should be small. We have compared the results for the conductance with and without SOC in the leads. As an example we show in Fig. 1 the comparison for the geometries discussed in Fig. 2 of the paper for $\phi = \pi/4$. We find that the neglect of SOC in the leads changes the contact resistance by a few percent, but leaves conclusions on the anisotropy properties of the conductance unchanged. In the presented calculations we have therefore neglected SOC in the leads.

The evolution of the contact during elongation (Fig. 2 of the paper) is simulated by means of classical molecular dynamics simulations in exactly the same way as it was done in Ref. [11]. We refer the reader to this reference for details.

II. IDEAL CONTACT GEOMETRIES: FE AND CO

Similar to the results in Fig. 1 of the paper we also analyzed ideal contacts of Fe and Co. We use the SOC constant $\xi_i = 70$ meV also for these materials.

In the case of Fe, the ideal contact is formed in the bcc [001] direction with atoms on bcc lattice sites [Fig. 2(a)]. Due to the large apex angle of the two pyramids forming the contact, the atom layers behind the central atoms give an important contribution to the conductance. This is why in this case we chose a dimer configuration as ideal geometry, in order to reduce this contribution. Note that again, although the absolute anisotropy amplitude of an individual channel exceeds $0.05e^2/h$, the anisotropy amplitude of the total conductance remains more than one order of magnitude smaller, below $0.004e^2/h$ (i.e. $\leq 0.08\%$ in relative conductance variation). Under a perturbation of the contact geometry [Fig. 2(b)], the conductance changes remarkably, due to the sensitivity of the d orbitals to the geometry. More strikingly, the absolute anisotropy amplitude of the conductance increases by roughly one order of magnitude to $0.05e^2/h$, a relative conductance variation of more than 2%. Again this follows from the notable robustness of the amplitude of the channel anisotropy against disorder and the fact that the individual channel contributions do not cancel entirely anymore.

Likewise we analyzed atomic contacts of Co. An example for a contact formed by two pyramids with one central atom grown in the hcp [001] direction is shown in Fig. 2(c). Here the total conductance shows a relative anisotropy amplitude of around 0.1%, this time with a maximum at $\theta = 0$ and quasi isotropic in ϕ. Again, the anisotropy amplitude of individual channels exceeds that of the total conductance by more than an order of magnitude. Under perturbation [Fig. 2(d)], the individual channel anisotropy amplitudes once again remain on the same order of magnitude but the different channel contributions do not cancel out anymore, leading to a relative anisotropy amplitude of 1% in the conductance. These findings support the general conclusions drawn based on the Ni contacts.

Note that recently Autès and coworkers [12] reported calculations for AMR in chains of Fe atoms between ideal surfaces. The main features of their results are in agreement with ours.

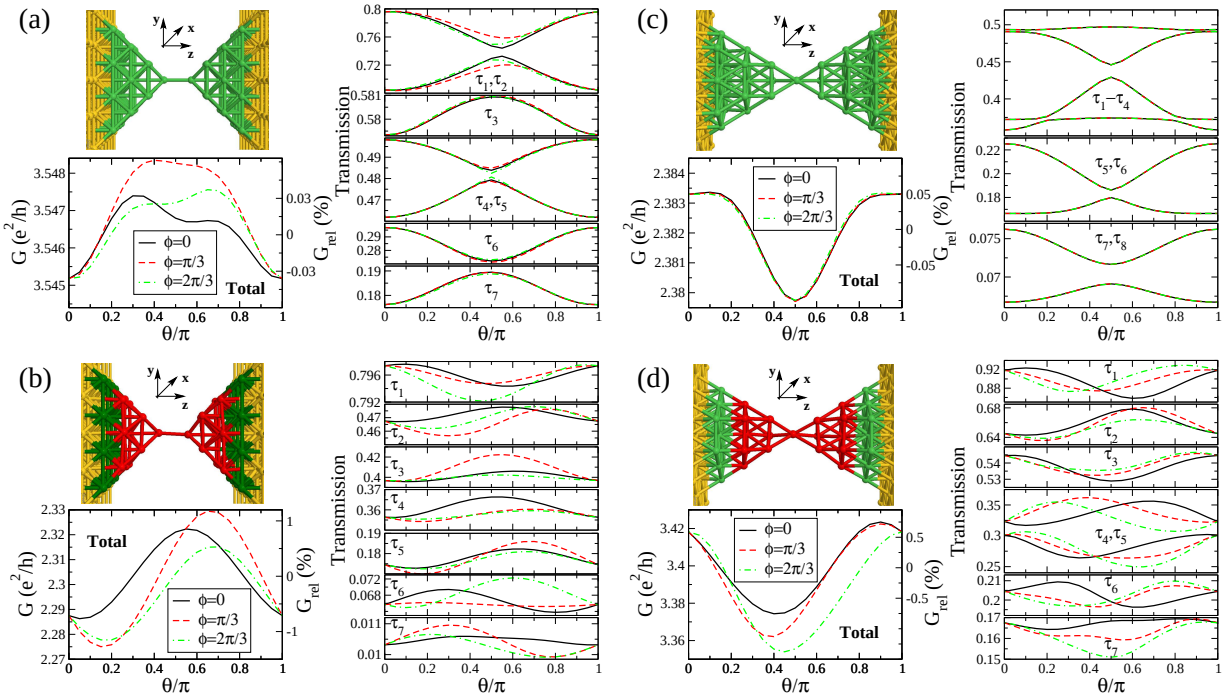

FIG. 2: (Color online) (a) The upper left panel shows a Fe dimer contact grown along the bcc [001] direction and with the atoms sitting on lattice positions. The green atoms are those in the atomic constriction, while the yellow ones are part of the surfaces used to model the leads. The lower left panel shows the total and relative conductance of this contact as a function of θ and for different azimuthal angles ϕ, while the right panel shows the corresponding channel decomposition. (b) The same as in (a), but for the geometry shown in the upper left panel, where the ideal contact of (a) has been distorted by changing randomly the atoms marked in the red by a maximum amplitude of 5% of the nearest-neighbor distance. (c,d) The same as in (a,b), but for a Co one-atom contact grown along the hcp [001] direction.

III. A MINIMAL CHAIN MODEL

A. Definition of the model

Here we study the effect of SOC in ferromagnetic atomic contacts of the $3d$ ferromagnets for an idealized model that captures the most essential aspects of the problem. We consider a contact formed by two linear, semi-infinite, parallel chains of identical atoms in $\vec{e}_z$ direction, joined in a central region consisting of the two tip atoms (see scheme in Fig. 3). To describe the electronic structure we consider a tight-binding model taking into account the E_2 subset of the d orbitals with $m_z = \pm 2$ containing the d_{xy} and $d_{x^2-y^2}$ orbitals. The onsite elements for the two spin orientations are assumed to be spin-split by Δ due to ferromagnetic order. The interatomic hopping integrals are restricted to nearest neighbors. In terms of Ref. 13, the only contributing hopping integral is of the $dd\pi$ type. The hoppings are assumed to be equal on all lead atoms but may differ between the two central atoms. Furthermore SOC with a finite coupling constant ξ is taken into account for the central atoms. In addition, we may include an "impurity" to one of the chains by modifying the hopping between two of its atoms. The used parameters are listed in Tab. I.

Quantity	Symbol	Value
Onsite energy (no splitting)	ε_0	0.0 eV
Spin-splitting	Δ	0.5 eV
Lead hopping $dd\pi$	π_l	1 eV
Center hopping $dd\pi$	π_c	0.4 eV
Impurity hopping $dd\pi$	π_s	0.8 eV
Spin-orbit coupling	ξ	0.2 eV

TABLE I: Parameters for the d_{E_2} orbitals chain with SOC in the central atoms.

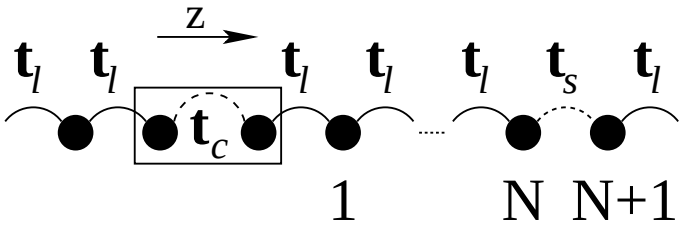

FIG. 3: Model system: linear chain of d orbitals (chain axis in z direction) eventually coupled to a distant impurity N sites away from the constriction.

In the absence of impurities, the term $\mathbf{H}^{(0)}$ in the Hamiltonian has the form

$$\mathbf{H}^{(0)} = \begin{pmatrix} \ddots & \ddots & 0 & 0 & 0 & 0 \\ \ddots & \mathbf{H}_0 & \mathbf{t}_l & 0 & 0 & 0 \\ 0 & \mathbf{t}_l & \mathbf{H}_0 & \mathbf{t}_c & 0 & 0 \\ 0 & 0 & \mathbf{t}_c & \mathbf{H}_0 & \mathbf{t}_l & 0 \\ 0 & 0 & 0 & \mathbf{t}_l & \mathbf{H}_0 & \ddots \\ 0 & 0 & 0 & 0 & \ddots & \ddots \end{pmatrix}. \tag{15}$$

The E_2 basis functions $\alpha = 1, 2$ are taken in the order d_{xy}, $d_{x^2-y^2}$. Then the diagonal blocks $\mathbf{H}_0 = \mathrm{diag}(\{\varepsilon_{\alpha\sigma}\})$ are of the form

$$\mathbf{H}_0 = \begin{pmatrix} \varepsilon_0 + \Delta/2 & 0 & 0 & 0 \\ 0 & \varepsilon_0 - \Delta/2 & 0 & 0 \\ 0 & 0 & \varepsilon_0 + \Delta/2 & 0 \\ 0 & 0 & 0 & \varepsilon_0 - \Delta/2 \end{pmatrix} \tag{16}$$

and the off-diagonal blocks are $\mathbf{t}_c = \pi_c \mathbf{1}$ and $\mathbf{t}_l = \pi_l \mathbf{1}$. Note that as the atoms lie on a straight line, there are no hopping elements coupling different types of orbitals. In the absence of SOC, this model thus represents four uncoupled linear chains.

Including SOC couples the chains. Equation (3) yields the SOC blocks $\mathbf{H}^{(SO)}_{i,i} = (\xi_i/2) \sum_{\mu\nu} R_{\mu\nu}(\theta, \phi) \mathbf{l}^{(\mu)} \otimes \boldsymbol{\tau}^{(\nu)}$, where the Pauli matrices

$$\boldsymbol{\tau}^{(1)} = \begin{pmatrix} 0 & 1 \\ 1 & 0 \end{pmatrix}, \quad \boldsymbol{\tau}^{(2)} = \begin{pmatrix} 0 & -i \\ i & 0 \end{pmatrix}, \quad \boldsymbol{\tau}^{(3)} = \begin{pmatrix} 1 & 0 \\ 0 & -1 \end{pmatrix}, \tag{17}$$

and the orbital angular momentum matrices $\mathbf{l}^{(\mu)}$ reduced to the minimal set of d_{E_2} orbitals are zero except for $\mathbf{l}^{(3)} = 2\boldsymbol{\tau}^{(2)}$. Here ξ_i is taken to be finite only on the atoms i belonging to C.

In order to calculate the current I and the nonlinear conductance $G(V) = dI/dV$ at finite bias voltages, we modify the onsite energies of the C part of $\mathbf{H}^{(0)}$. Thus the current is obtained from Eq. (7) where

$$\mathbf{G}_{CC}(\varepsilon, V) = \left[\begin{pmatrix} (\varepsilon^+ - eV/2)\mathbf{1} - \boldsymbol{\Sigma}(\varepsilon - eV/2) & 0 \\ 0 & (\varepsilon^+ + eV/2)\mathbf{1} - \tilde{\boldsymbol{\Sigma}}(\varepsilon + eV/2) \end{pmatrix} - \mathbf{H}^{(0)}_{CC}(V = 0) - \mathbf{H}^{(SO)}_{CC} \right]^{-1}. \tag{18}$$

Here $\boldsymbol{\Sigma}(\varepsilon) = \mathrm{diag}(\{\Sigma_{\alpha\sigma}(\varepsilon)\})$ is a diagonal self-energy matrix arising from the coupling to the left C atom to the four independent, semi-infinite, homogeneous chains [14, 15]. It is of the form

$$\boldsymbol{\Sigma}(\varepsilon) = \mathbf{t}_l \mathbf{g}_0(\varepsilon) \mathbf{t}_l \tag{19}$$

where the Green's function of the "surface" satisfies $\mathbf{g}_0(\varepsilon) = [\varepsilon - \mathbf{H}_0 - \mathbf{t}_l \mathbf{g}_0(\varepsilon) \mathbf{t}_l]^{-1}$. The resulting self-energy components are all of the form $\Sigma_{\alpha\sigma}(\varepsilon) = \pi_l e^{i\Phi_{\alpha\sigma}}$, with $\cos\Phi_{\alpha\sigma} = (\varepsilon - \varepsilon_{\alpha\sigma})/2\pi_l$, where π_l is the hopping integral. In the absence of the impurity, the self energy $\tilde{\boldsymbol{\Sigma}}(\varepsilon)$ for the right-hand C atom is equal to $\boldsymbol{\Sigma}(\varepsilon)$. The modifications due to the introduction of the impurity are discussed below in more detail.

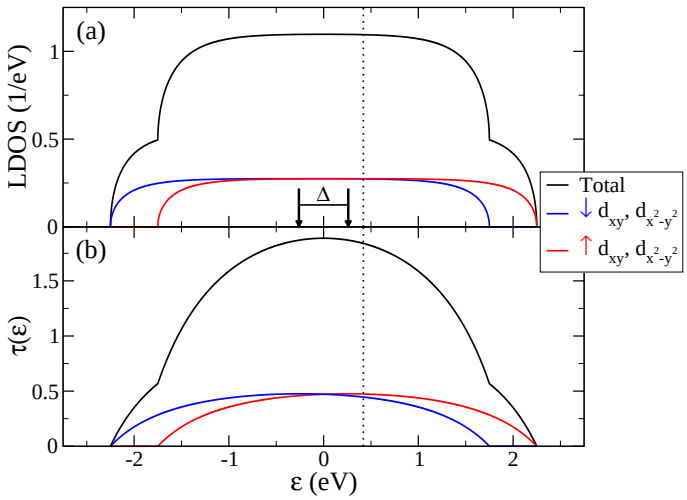

FIG. 4: (Color online) Linear chain of d_{E_2} orbitals in absence of SOC: (a) LDOS of the tip atoms projected on the orbitals and (b) total transmission and its channel decomposition. The position of ε_F is indicated with a dotted line.

B. Results: No spin-orbit coupling and no impurity

Let us first discuss the results in the absence of SOC, in which case there are four independent linear chains. The local density of states (LDOS) $\rho_{\alpha\sigma}(\varepsilon)$ projected onto the orbital $\alpha\sigma$ of one of the tip atoms is as for two half-infinite chains linked by a weaker hopping and given by

$$\rho_{\alpha\sigma}(\varepsilon) = -\frac{1}{\pi}\,\mathrm{Im}\left\{\frac{\varepsilon - \varepsilon_{\alpha\sigma} - \Sigma_{\alpha\sigma}(\varepsilon)}{\pi_c^2 - [\varepsilon - \varepsilon_{\alpha\sigma} - \Sigma_{\alpha\sigma}(\varepsilon)]^2}\right\}, \tag{20}$$

Here, the spin-dependent onsite energies are $\varepsilon_{\alpha\sigma} = \varepsilon_0 \pm \Delta/2$ for majority/minority spin, and the center hopping elements π_c are the corresponding two center integrals. The resulting LDOS for the different orbitals is shown in Fig. 4.

In the real $3d$ materials ε_F lies close to the edge of the d bands. In this one-dimensional model we choose ε_F to be well within the bands to avoid the singularities at the band edges, which are particular to one-dimensional ideal chains. We choose $\varepsilon_F = 0.42$ eV (see Fig. 4).

Next, let us have a look at the transmission function for the system of four independent chains. The transmission $\tau_{\alpha\sigma}$ for the chain of orbital $\alpha\sigma$ reads (within the band):

$$\tau_{\alpha\sigma}(\varepsilon) = \frac{[\Gamma_{\alpha\sigma}(\varepsilon)]^2\,\pi_c^2}{\left|\pi_c^2 - [\varepsilon - \varepsilon_{\alpha\sigma} - \Sigma_{\alpha\sigma}(\varepsilon)]^2\right|^2}, \tag{21}$$

where we introduced $\Gamma_{\alpha\sigma}(\varepsilon) = -2\,\mathrm{Im}\,[\Sigma_{\alpha\sigma}(\varepsilon)]$. These transmission functions are plotted in Fig. 4. In absence of impurities in the leads, the transmission curves as a function of energy are structureless. At the Fermi energy the transmission of the two-fold degenerate channels is 0.474 (0.446) for majority (minority) spins.

C. Results: spin-orbit coupling

When we add the SOC, the resulting LDOS and conductance curves are shown in Fig. 5. Note the large anisotropy amplitude in the conductance channels, which can be up to $0.08e^2/h$. Due to the rotational symmetry of the linear chain, the transmission probabilities are independent of the azimuthal angle ϕ. The channel anisotropies with respect to θ balance to a high degree, leading to a very small anisotropy amplitude of the total conductance, on the order of $0.005e^2/h$. At $\theta = \pi/2$ the conductance channels cross and are two-fold degenerate. In the full basis of the five d orbitals, the orbital angular momentum matrices $\mathbf{l}^{(1)}$ and $\mathbf{l}^{(2)}$ would be non-zero and couple the E_2 doublet to the other d orbitals, which would lift this degeneracy. This behavior is similar to the properties of ideal contacts geometries of Fe and Co in Fig. 2 and of Ni in Fig. 1 of the paper.

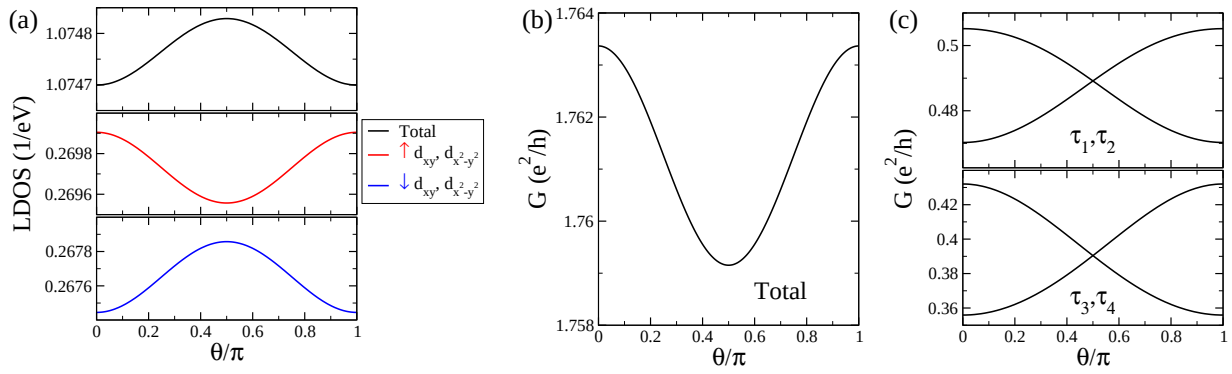

FIG. 5: (Color online) Linear chains of d_{E_2} orbitals with SOC in the tip atoms: (a) LDOS at the Fermi energy projected on the orbitals, (b) total conductance and (c) channel decomposition.

D. Description of impurities

In order to describe the conductance oscillations due to quantum interference, we may place an impurity in one of the leads, far away from the center. We choose to place it in the right lead, and model it by a modified hopping $\mathbf{t}_s$ between the N th and the $(N+1)$ th atom in this lead.

The lead self energy modified by the impurity is of the form $\tilde{\mathbf{\Sigma}}(\varepsilon)$ reads

$$\tilde{\mathbf{\Sigma}}(\varepsilon) = \mathbf{t}_l \tilde{\mathbf{g}}_0(\varepsilon) \mathbf{t}_l \tag{22}$$

where $\tilde{\mathbf{g}}_0(\varepsilon) = \tilde{\mathbf{g}}_{1,1}(\varepsilon)$ is the "surface" component of the impurity-modified lead Green's function $\tilde{\mathbf{g}}(\varepsilon)$. Placing now the impurity N sites away from the tip atom as indicated in Fig. 3, we find

$$\tilde{\mathbf{g}}_{1,1}(\varepsilon) = \mathbf{g}_{1,1}(\varepsilon) + \mathbf{g}_{1,N}(\varepsilon)\mathbf{t}_s \left(\mathbf{g}_0^{-1}(\varepsilon) - \mathbf{t}_s \mathbf{g}_{N,N}(\varepsilon)\mathbf{t}_s\right)^{-1} \mathbf{t}_s \mathbf{g}_{N,1}(\varepsilon). \tag{23}$$

Here $\mathbf{t}_s = \pi_s \mathbf{1}$ is the modified hopping modelling the impurity (with a reduced hopping integral π_s), $\mathbf{g}_0(\varepsilon)$ is as in eq. 19, and the Green's functions $\mathbf{g}_{1,N}(\varepsilon)$, $\mathbf{g}_{N,1}(\varepsilon)$, $\mathbf{g}_{1,1}(\varepsilon)$, and $\mathbf{g}_{N,N}(\varepsilon)$ are those of the uncoupled N atom chain located between the center and the impurity. They are diagonal in the indices $(\alpha\sigma)$ and may be calculated analytically, with the results

$$\{\mathbf{g}_{1,1}\}_{\alpha\sigma,\alpha\sigma} = \{\mathbf{g}_{N,N}\}_{\alpha\sigma,\alpha\sigma} = \frac{\sin N\Phi_{\alpha\sigma}}{\pi_l \sin(N+1)\Phi_{\alpha\sigma}}, \quad \{\mathbf{g}_{1,N}\}_{\alpha\sigma,\alpha\sigma} = \{\mathbf{g}_{N,1}\}_{\alpha\sigma,\alpha\sigma} = \frac{\sin \Phi_{\alpha\sigma}}{\pi_l \sin(N+1)\Phi_{\alpha\sigma}} \tag{24}$$

where $\Phi_{\alpha\sigma}$ is again defined through $\cos\Phi_{\alpha\sigma} = (\varepsilon - \varepsilon_{\alpha\sigma})/2\pi_l$. The resulting self energies remain diagonal in $(\alpha\sigma)$ and are in general oscillating functions of ε with an oscillation period proportional to the distance of the impurity from the center. By placing the impurity $N = 751$ sites from the constriction, the results presented in Fig. 3 of the paper are obtained.

[1] M. J. Mehl and D. A. Papaconstantopoulos, Phys. Rev. B **54**, 4519 (1996).
[2] http://cst-www.nrl.navy.mil/bind/.
[3] H. Takayama, K.-P. Bohnen, and P. Fulde, Phys. Rev. B **14**, 2287 (1976).
[4] J. C. Cuevas, A. L. Yeyati, and A. Martín-Rodero, Phys. Rev. Lett. **80**, 1066 (1998).
[5] M. Häfner *et al.*, Phys. Rev. B **70**, 241404 (2004).
[6] M. Brandbyge, N. Kobayashi, and M. Tsukada, Phys. Rev. B **60**, 17064 (1999).
[7] M. Dreher *et al.*, Phys. Rev. B **72**, 075435 (2005).
[8] J. K. Viljas, J. C. Cuevas, F. Pauly, and M. Häfner, Phys. Rev. B **72**, 245415 (2005).
[9] M. Häfner *et al.*, Phys. Rev. B **77**, 104409 (2008).
[10] F. Guinea, C. Tejedor, F. Flores, and E. Louis, Phys. Rev. B **28**, 4397 (1983).
[11] F. Pauly *et al.*, Phys. Rev. B **74**, 235106 (2006).
[12] G. Autès, C. Barreteau, D. Spanjaard, and M.-C. Desjonquères, Phys. Rev. B **77**, 155437 (2008).
[13] J. C. Slater and G. F. Koster, Phys. Rev. **94**, 1498 (1954).
[14] D. M. Newns, Phys. Rev. **178**, 1123 (1969).
[15] P. W. Anderson, Phys. Rev. **124**, 41 (1961).